# Colloid retention and mobilization mechanisms under different physicochemical conditions in porous media: A micromodel study

Safna Nishad, Riyadh I. Al-Raoush

Powder Technology 377 (2021) 163–173

Contents lists available at ScienceDirect

Powder Technology

journal homepage: www.elsevier.com/locate/powtec

# Colloid retention and mobilization mechanisms under different physicochemical conditions in porous media: A micromodel study

Safna Nishad, Riyadh I. Al-Raoush *

*Department of Civil and Architectural Engineering, Qatar University, P.O Box 2713, Doha, Qatar*

ARTICLE INFO

*Article history:*
Received 26 May 2020
Received in revised form 20 August 2020
Accepted 26 August 2020
Available online 1 September 2020

*Keywords:*
Colloid retention
Colloid mobilization
Micromodel
Pore-scale visualization
Solution chemistry
Hydrophobicity

ABSTRACT

Clear understanding of pore-scale mechanisms that control transport and retention of colloids in porous media at different physicochemical conditions is critical to improve design and efficient cleanup methodologies of filter beds. The objective of this work was to investigate the impact of hydrophobicity, solution ionic strength, and pH on colloid retention mechanisms in single-phase and two-phase flow in porous media systems. A series of experiments were conducted using a geometrically representative micromodel. Hydrophilic and hydrophobic colloids were dispersed in water at different solution ionic strength and pH conditions. Findings indicate that hydrophilic colloids exhibit high filtration efficiency as the colloids interact attractively with other colloids and solid-water-interface irrespective of the solution chemistry. However, for hydrophobic colloids, changes in solution chemistry significantly increase colloid retention where the colloid interaction become attractive with the increase in ionic strength and decrease in pH values. Colloids attached to the collector surfaces mobilized by the strong capillary forces induced by the moving gas-water interface and transported along with the interface. However, hydrophilic colloids redeposited on gas-water-solid interfaces or thin water films because of their greater capillary potential. Therefore, greater filtration efficiency is achieved with the hydrophilic colloids compared to the hydrophobic colloids for which the efficiency can be improved by changing the solution chemistry. Moreover, the removal efficiency by the moving gas-water interface was observed to be more for hydrophobic colloids compared to hydrophilic colloids for which the efficiency can be improved by lowering the ionic strength or increasing the pH value. This study indicates that the coupled effects of solution chemistry and colloid hydrophobicity should be taken into account while investigating efficient filtration and cleaning practices for the filter beds.



## 1. Introduction

While deep bed filters have been widely adopted for water purification and wastewater treatment processes, the associated pore-scale mechanisms related to the transport and retention of colloids in the pore space of the porous media are still poorly understood [1,2]. Especially, surface interactions of colloids in water treatment processes where colloids may consist of heavy metals, pesticides, or other pollutants such as bacteria and viruses [3,4]. Previous column experiments emphasized the impact of various factors that govern the transport and retention of colloids in porous media such as colloid hydrophobicity, solution ionic strength, and solution pH on the colloid deposition efficiency [5–7]. The lack of visualization evidence limits prediction accuracy and better understanding of related mechanisms [5,6,8]. The efficiency of colloid removal from the pore-space of filter beds is an active area of research where the need to better understand mobilization of colloids by the moving Gas-Water-Interfaces (GWI) is essential to better predict filter beds performance and efficiency [9–12]. However, the impact of physical and chemical factors on the mobilization mechanisms of colloids is still unclear. Therefore, a clear understanding of the interactions between colloids and the collectors or GWI under various physical and chemical conditions is essential to accurately predict the efficiency of filtration and cleaning of filter beds.

Column and core flooding experiments have been conducted to understand the behavior of colloid transport in saturated porous media coupled with the DLVO interaction energies [2,8–11]. Such studies have focused mainly on the impact of type, shape, and concentration of colloid, solution chemistry, and flow velocity on colloid breakthrough concentrations. Estimates of colloid attachment on collector surfaces were obtained by investigating breakthrough concentrations and surface interaction energies at different experimental conditions. For the repulsive surface interactions, straining was the major suggested retention mechanism in those studies [2,8–11]. For instance, attachment on the collector surfaces was predicted to be significant for colloids under high ionic strength and smaller retention on grain-grain contacts or pore-constrictions for colloids under lower ionic strength conditions.

* Corresponding author.
*E-mail address:* riyadh@qu.edu.qa (R.I. Al-Raoush).

https://doi.org/10.1016/j.powtec.2020.08.086

However, the lack of pore-scale visualization of those studies limits the fundamental understanding of pore-scale mechanisms of colloid transport and retention in porous media.

Micromodels fabricated using different materials such as silica, glass, polydimethylsiloxane (PDMS) have been used to represent porous media systems [6,10,13–16]. The transparency of such materials allows direct visualization of the relevant pore-scale processes that take place during transport experiments using optical microscopy. Highly controllable physical and chemical environments in the micromodel enhance their applicability to focus on relevant and interested experimental conditions. The clogging behavior of colloids was investigated using microfluidic channels or micromodels with homogenous geometry as a function of the relative size of colloid and pore throat size, colloid concentration, flow velocity, and ionic strength [17–21]. Direct pore-scale visualization obtained from those studies revealed important mechanisms such as size exclusion, pore bridging, and the progressive clogging of the pore throats in the porous media in real-time. However, surface interactions and colloid attachment on the collector surfaces have not been considered while investigating the transport of colloids in porous media.

Experiments on colloid covered surfaces and capillary channels were conducted to study the mobilization of colloids from Solid-Water-Interface (SWI) by the moving GWI [11,12,13,22,23]. Hydrophilic or hydrophobic colloids deposited on glass slides were mobilized by drainage or imbibition fronts to observe the colloid removal by the moving GWI. Theoretical conceptualizations were developed based on microscopic observations by incorporating forces acting on colloids at the three-phase contact point. Variations in the release behavior of hydrophilic and hydrophobic colloids by the drainage and imbibition fronts were explained by the capillary force acting on the colloid at the contact point. However, the kinetics of colloid deposition and gas-phase transport in porous media were not observed in these micro-fluidic experiments.

A series of two-phase flow experiments were conducted to study the impact of colloid hydrophobicity, fluid interfacial tension, and fluid saturation on colloid retention and mobilization [6,15,24]. Micromodels with a triangulated network of pores were used and breakthrough curves of colloids were measured at the outlet channel using a confocal microscope. While these studies were helpful to explain certain aspects of colloids behavior in a hydrophobic micromodel, the simplified geometry of the micromodel was considered as a limitation.

Several studies have used micromodels that incorporated real sand-stone geometry obtained from computer tomography images to investigate several applications such as hydrocarbon recovery, $CO_2$ sequestration, and specific biomedical applications [25–32]. These studies have focused on multiphase flow through porous media and related pore-scale processes such as capillary pressure, relative permeability, and residual saturation using the captured images obtained from micromodels. While a few studies were conducted on clay functionalized micromodels to estimate oil recovery in response to low salinity flooding [20,21], micromodels with physically representative geometry have not been used to study colloid transport in porous media.

Previous studies on colloid transport in porous media lack visualization evidence on the processes that take place in the pore-scale. To the best of authors' knowledge, the coupled impact of colloid type, solution ionic strength, and pH on colloid retention and mobilization has not been investigated at the pore-scale. Understanding colloids behavior at the pore-scale allows better design of filters for improved efficiency and better colloid removal practices.

The objective of this work was to investigate the impact of hydrophobicity, solution ionic strength, and pH on colloid retention mechanisms in single-phase and two-phase flow in porous media systems. A series of experiments were conducted using a hydrophilic glass micromodel with physically representative geometry. Hydrophilic and hydrophobic colloids were dispersed in water with different solution ionic strength and pH conditions. The captured images during single and two-phase flow were used to better understand retention and mobilization mechanisms in porous media.

## 2. Materials and methods

### 2.1. Materials

A microfluidic chip etched on a borosilicate glass represented the porous medium (Micronit Micro Technologies B.V., Netherlands) with an area of 20 mm × 10 mm and a depth of 20 μm. The surface of the microfluidic channel was hydrophilic, with an average contact angle 15°–25° (Manufacturer's data). The pore volume, porosity, and permeability of the micromodel were 2.3 μL, 0.58, and 2.5 Darcy, respectively. The microfluidic chip, holder, and the tube connections are shown in Fig. 1-a and the segmented image of the entire chip in Fig. 1b.

The colloids used in this study were Polystyrene (Hydrophobic PS) and Carboxylate Modified PolyStyrene (Hydrophilic CMPS) (Magsphere Inc., Pasadena, CA) with a mean diameter of 5 μm and a density of 1.05 g/cc. Colloid suspensions of 0.5% concentration were prepared in brine with approximately $7.3 \times 10^7$ colloids/mL. The diluted suspensions were sonicated in a water bath for 30 min before each experiment using an ultrasonic processor (SONICS, Vibra cell) to obtain a monodispersed colloidal suspension. Zeta potential values of the colloids with different solution chemistry used in this study were measured with Zetasizer (Nano ZSP, Malvern Panalytical, Southborough, MA) at 21 °C. The experimental conditions used in this study are given in Table 1.

Brine and Carbon dioxide ($CO_2$) gas were the two immiscible fluids used in this study. The ionic strength of the brine was changed by adding NaCl, and the pH was adjusted by adding 0.1 M HCl or 0.1 M NaOH.

### 2.2. Experimental setup

Fig. 1c shows a schematic of the experimental setup. The micromodel was placed on a microscope stage (Leica Z6 APO), and the inlet port of the micromodel was connected to a precision syringe pump (Kats Scientific, NE-1010) to inject brine along with colloids. Another port of the micromodel was connected to a Teledyne ISCO pump (500 HP) for $CO_2$ injection at constant pressure (10 ± 1 kPa) and room temperature (21 ± 1 °C). The injection pressure was achieved using a high-sensitivity diaphragm-sensing pressure-reducing regulator (Swagelok co), and the pressure was monitored with a pressure transducer (OMEGA PX309-100GV). A commercial $CO_2$ cylinder (Buzwairgas, 99.99%) supplied the $CO_2$ gas to the ISCO pump. An inline filter was connected to the micromodel to prevent the flow of colloids to the pressure regulator. The flow processes in the micromodel were observed using a high-resolution camera (Leica MC170 with a resolution of 5 Mpixels) attached to the microscope with image and video capturing function controlled by a computer. The resolution of the acquired images of the experiments was 0.94 μm/pixel.

The experimental system, including micromodel, tubing, and other components, was cleaned before each test by injecting 100 Pore Volumes (PV) of ethanol followed by 500 PVs of deionized water. The micromodel was dried at 80 °C for 48 h and was assembled with all components (Fig. 1c) at room temperature (21 ± 1 °C). The trapped air and ions inside the micromodel were displaced by injecting several PVs of deionized water. For each experiment, the micromodel was initially saturated with a colloid-free brine solution that would carry the colloids at later steps in the experiments. The colloidal suspension was then injected into the micromodel carefully to avoid inlet clogging. Images of the micromodel saturated with colloids were captured at the end of this step. Then, the system was pressurized using the ISCO pump up to 10 kPa by injecting $CO_2$ at constant pressure to avoid the effect of change in pressure on colloid migration. While maintaining the

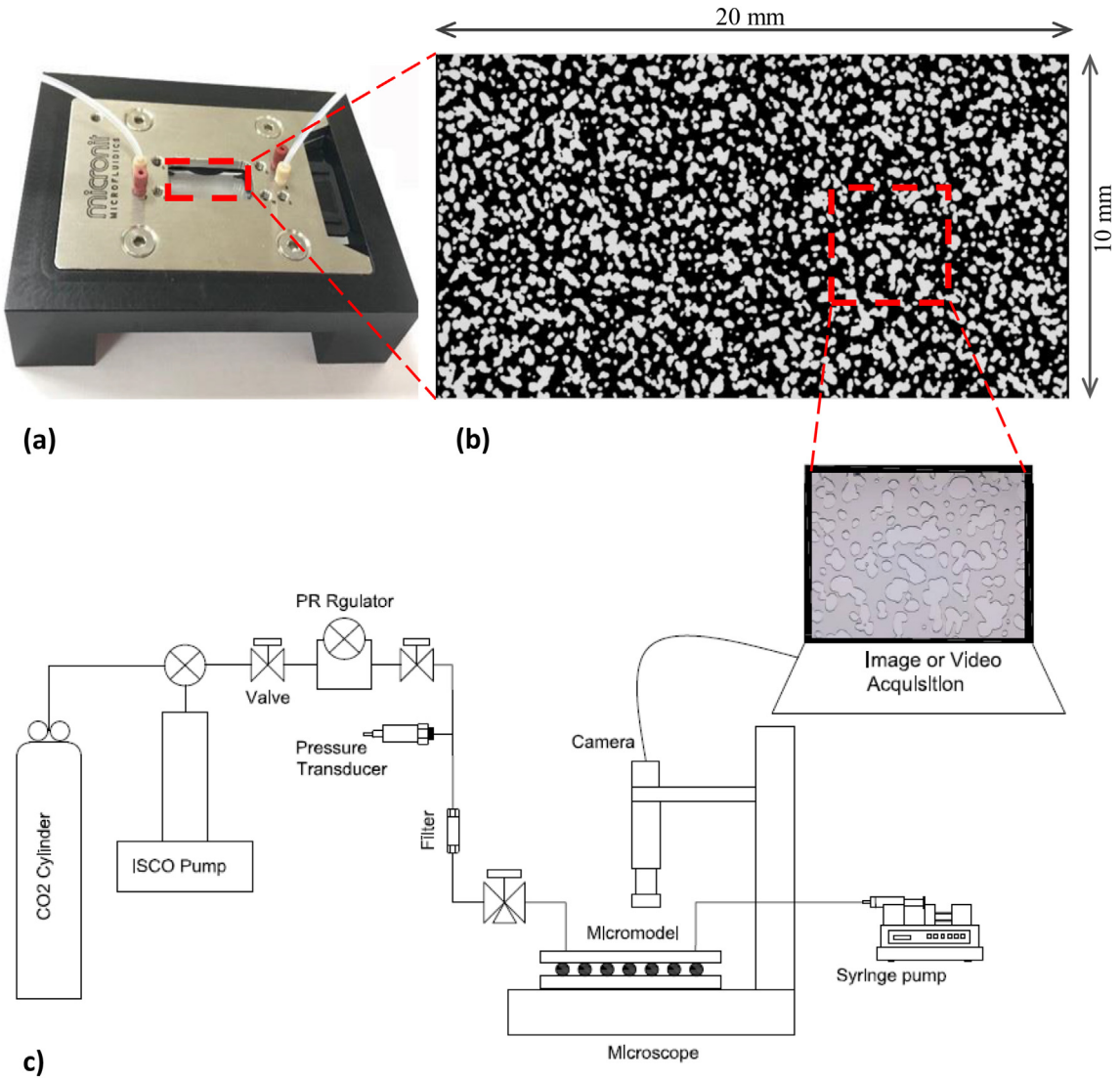


**Fig. 1.** (a) The Microfluidic chip, holder and connections used in this study; (b) Segmented image of the entire chip used in this study (black pore space and white solid phase); (c) Schematic diagram of the experimental set up (Note: Figure not drawn to scale).

**Table 1**
List of experimental conditions used in this study and masses of colloids retained in the micromodel.

| Experiment no. | Colloid | Solution ionic strength (mM) | Solution pH | Zeta potential (mV) | Initial colloid content (% of pore space) | The ratio of retained mass after drainage to the initial colloid content (%) | The ratio of retained mass on GWI to the initial colloid content (%) | The ratio of retained mass on GWI to the total mass retained after drainage (%) |
|---|---|---|---|---|---|---|---|---|
| PS1 | Hydrophobic PS | 0 | 7 | −35.00 | 2.47 | 5.9 | 3.4 | 57.7 |
| PS2 | | 1 | 4 | −31.40 | 1.63 | 29.8 | 25.93 | 87.0 |
| PS3 | | 1 | 10 | −38.00 | 3.00 | 7.7 | 5.52 | 71.7 |
| PS4 | | 100 | 4 | −12.74 | 3.50 | 62.6 | 38.43 | 61.4 |
| PS5 | | 100 | 10 | −29.90 | 1.23 | 35.7 | 28.92 | 81.0 |
| CMPS1 | Hydrophilic CMPS | 0 | 7 | −15.20 | 4.41 | 76.9 | 34.5 | 45.1 |
| CMPS2 | | 1 | 4 | −3.60 | 2.08 | 77.6 | 54.32 | 70.0 |
| CMPS3 | | 1 | 10 | −10.40 | 1.92 | 47.8 | 28.3 | 59.2 |
| CMPS4 | | 100 | 4 | −3.47 | 2.17 | 90.0 | 47.88 | 53.2 |
| CMPS5 | | 100 | 10 | −5.28 | 2.38 | 56.9 | 38.4 | 67.5 |

pressure in the network, brine was drained at a rate of 10 μL/min (mean pore water velocity of 5.2 m/h, Capillary number, $Ca = 3.2 \times 10^{-7}$). Images and videos of colloid mobilization during two-phase flow and their retention on different interfaces were captured. The captured images were processed to obtain the percentage of colloids retained in the micromodel after each phase of the experiment. Image processing techniques adopted in this study are documented in the Supporting Material. Interfaces of interest include Solid-Water interfaces (SWI), Gas-Water Interfaces (GWI), Gas-Water-Solid Interfaces (GWSI), and thin films.

## 3. Results and discussions

Ten sets of experiments were conducted at the experimental conditions given in Table 1. Each experiment was conducted under single and two-phase flow. Colloid masses retained in the pore-space after single and two-phase flow were determined from the captured images using image processing and are shown in Table 1. Table 2 summarizes the observed interactions at different experimental conditions.

### 3.1. Colloid retention mechanisms in single-phase flow

Fig. 2 shows pore-scale images of size, 2.0 mm × 1.5 mm (2127 × 1595 pixels) at different experimental conditions given in Table 1. The captured images reveal that two colloid interactions take place in single-phase flow, namely colloid–colloid and colloid-SWI interactions. The significance of these two mechanisms greatly influenced by the ionic strength, pH, and type of colloid, as will be discussed in detail in the following sections.

#### 3.1.1. Colloid-colloid interaction

Pore-scale images given in Fig. 2 show three distinct mechanisms of colloid-colloid interactions identified in single-phase flow, namely (a) repulsive interaction (RI) that leads to formation of dispersed colloids in the pore space (b) short-range interaction (SRI) that leads to the development of small flocs near the solid surface only and (c) long-range interaction (LRI) that leads to the formation of larger colloidal aggregates.

Repulsive interactions, RI, were observed for hydrophobic colloids at low ionic strength or high pH conditions (Fig. 2a, c, e and i). On the other hand, short-range interactions, SRI, were observed near the solid surfaces at high ionic strength and low pH case (Fig. 2g). Additionally, hydrophilic colloids at low ionic strength and high pH exhibited SRI (Fig. 2b and f). Long-range interactions, LRI, were observed only for hydrophilic colloids at high solution ionic strength or low pH (Fig. 2d, h, and j).

High stability of hydrophobic colloids observed in this study contradicts previous studies that suggested enhanced aggregation of hydrophobic colloids due to hydrophobic interaction among colloids [6,33]. Visual observations confirm the role of the magnitude of measured zeta potential on the colloid stability trend observed in this study, which is in agreement with previous studies [34,35]. Accordingly, the lower magnitude of zeta potential of hydrophilic colloids explains their instability compared to the hydrophobic colloids. Zeta potential values given in Table 1 at different conditions range from −3.47 mV to −38 mV. Zeta potential values show a good agreement with the general trend that the magnitude decreases as the ionic strength increases or as pH decreases. The type of colloid interactions revealed from pore-scale images at different conditions shown in Fig. 2 can be linked to their zeta potential values given in Table 1. As shown in Fig. 2, RI interactions were observed in systems where zeta potential value greater than 30 mV whereas LRI were observed in systems where zeta potential less than 6 mV. SRI were observed in systems of zeta potential values between 6 mV and 30 mV.

The interaction energy profile of the colloids computed from the DLVO theory (Supplementary_Fig. S2) and the estimated energy minima and energy barrier values (Supplementary Table S1) aid to explain the interaction mechanisms discussed above.

In systems CMPS2, CMPS4, and CMPS5, pore-scale images show significant colloid aggregation, and thus LRI was observed (Fig. 2d, h, and j). This observation was supported by the DLVO profiles, where the energy barrier between the colloids was negligible (Supplementary Fig. S2b). At later stages of the experiments, colloid aggregation was distributed primarily due to diffusion among colloids. Therefore, the small energy barrier (i.e., less than 5 kBT) can be overcome by the diffusion kinetic energy as observed in the CMPS2 system (Fig. 2d and Supplementary Table S1) [37,38]. However, the coexistence of the energy barrier and primary minima (at short-separation distance) on the energy profile indicates that SRI dominates where colloids overcome the repulsive barrier to interact with other colloids in strong primary minimum. For instance, as can be seen from Fig. 2b and f, a greater repulsive peak for CMPS1 and CMPS3 systems (Supplementary Fig. S2 and Supplementary Table S1) was overcome by the collision of dispersed colloids in bulk water with the deposited colloids on SWI. Therefore, the infusion of greater concentration of colloids at lower velocity can induce colloid aggregation on the collector surfaces due to particle Brownian motion for longer residence time.

Moreover, understanding colloid interaction mechanisms is critical to better predict their retention in filter beds. For instance, colloids that exhibit RI remain dispersed in the pore-space, which in turn reduces their retention in the porous media. On the other hand, pore bridging and larger aggregate formation take place in systems where colloids exhibit SRI and LRI, respectively, which may eventually cause clogging of small pore throats. The progressive or rapid clogging of the pore-space due to SRI or LRI may lead to permeability decrease and consequently reduced efficiency of filters. Therefore, understanding the interaction mechanisms helps to design efficient filters and suggest techniques for efficient cleaning practices.

#### 3.1.2. Colloid-SWI interaction

Three distinct colloid-SWI interaction mechanisms were observed, as shown in Fig. 2, namely (a) repulsive interaction (RI) that leads to suspension of colloids in bulk water (b) short-range interaction (SRI) that leads to the attachment of colloids only at the bottom of the micromodel and (c) long-range interaction (LRI) that leads to the colloid attachment on solid surfaces. Although the micromodel bottom is considered as a solid surface, it is the interaction separation distance that distinguishes SRI from LRI. For SRI, the attachment occurs only when the colloids are in close contact with the solid surface (i.e., at a very short separation distance). Sedimentation of colloids, while the flow ceased before the two-phase flow, created SRI of colloids with the micromodel bottom. In other words, colloids that exhibited LRI were attracted by the solid surface (either grain surfaces or micromodel bottom/top) during the flow of colloid suspension through the porous media. Hydrophobic colloids

**Table 2**
Summary of interactions of colloids at various conditions.

| IS (mM) | Hydrophobic colloids | | | | | Hydrophilic colloids | | | | |
|---|---|---|---|---|---|---|---|---|---|---|
| | 0 | 1 | | 100 | | 0 | 1 | | 100 | |
| PH | 7 (PS1) (a) | 4 (PS2) (c) | 10 (PS3) (e) | 4 (PS4) (g) | 10 (PS5) (i) | 7 (CMPS1) (b) | 4 (CMPS2) (d) | 10 (CMPS3) (f) | 4 (CMPS4) (h) | 10 (CMPS5) (j) |
| C-C (Fig. 2) | RI | RI | RI | SRI | RI | SRI | LRI | SRI | LRI | LRI |
| C-SWI (Fig. 2) | RI | SRI | RI | LRI | SRI | LRI | LRI | LRI | LRI | LRI |
| C-GWI (Fig. 3) | CR/HI | CR | CR/HI | CR | CR | CR | CR | CR | CR | CR |
| C-GWSI/Thin film (Fig. 5) | S | S | S | CR | CR | CR | CR | CR | CR | CR |

RI: Repulsive Interaction; SRI: Short-Range Interaction; LRI: Long-Range Interaction; CR: Capillary Retention; CR/HI: Capillary Retention/Hydrophobic Interaction; S: Straining only.

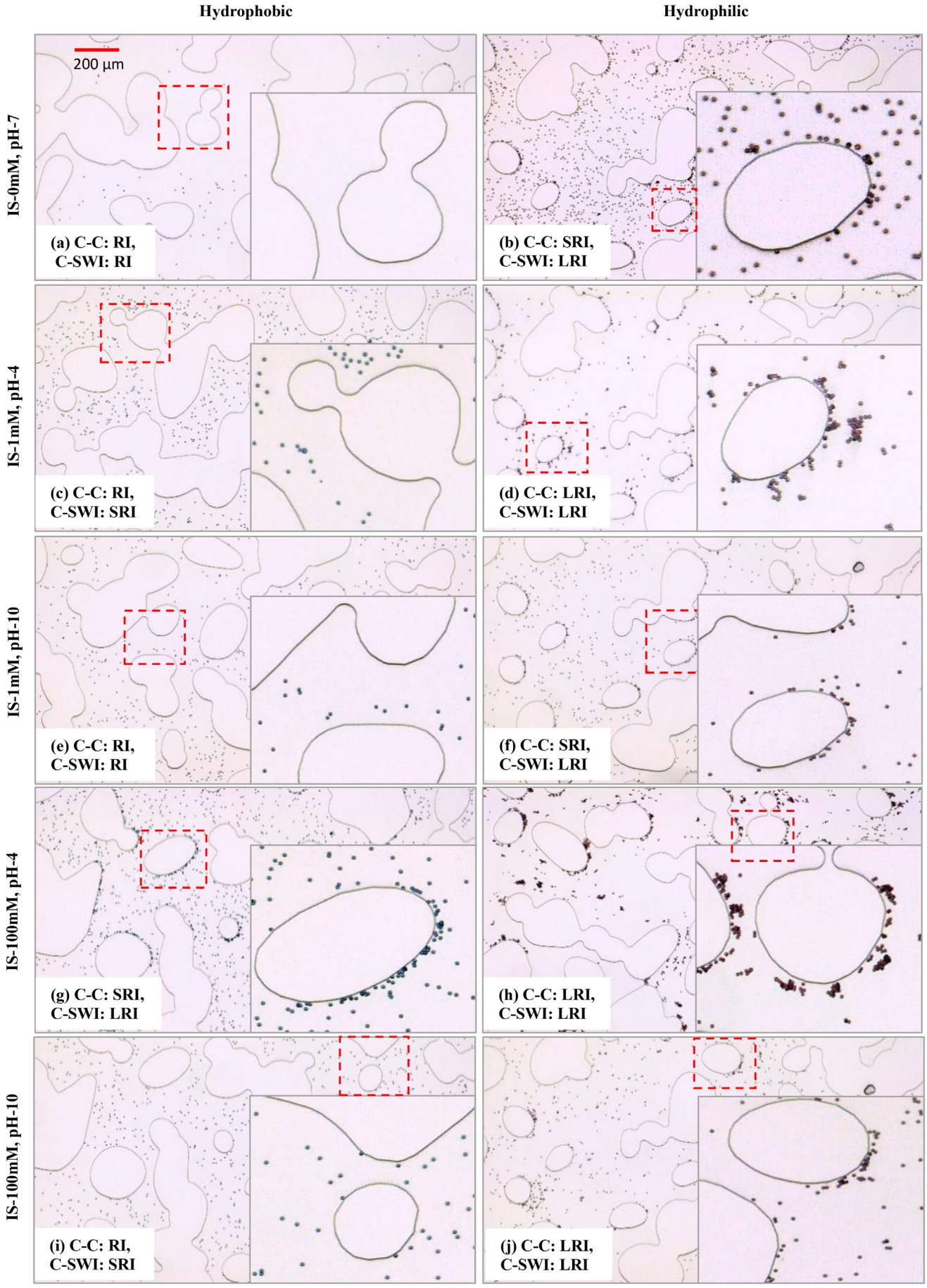


**Fig. 2.** Colloid interactions in Single-Phase flow at different experimental conditions. RI: Repulsive Interaction, SRI: Short-Range Interaction, LRI: Long-Range Interaction.

exhibited a wide range of interaction mechanism varying from RI to LRI, in contrast to the hydrophilic colloids, where they showed only LRI irrespective of the solution chemistry.

Previous studies suggested colloid interactions on SWI are independent of solution chemistry under favorable attachment conditions (i.e., the colloid and solid surface have opposite surface charges [36–38]). However, pore-scale observations show that although hydrophilic colloids and solid surfaces used in this study were negatively charged, favorable attachment conditions were observed when the surface charge of the colloid was close to zero, as given in Table 1 (i.e., less than 15 mV).

As shown in Fig. 2, hydrophobic colloids show a clear trend of the dependence of colloid attachment on solution chemistry (both ionic strength and pH). This observation is consistent with previous studies that show colloids under unfavorable attachment conditions (i.e., same surface charge) were retained at high ionic strength conditions [31,32]. However, Fig. 2c shows colloid attachment at the bottom of the micromodel at low ionic strength, where the colloid-SWI interaction became SRI due to low pH (for PS2). For those cases, the primary minimum at shorter separation distance results in the attachment of colloids that come closer to SWI by sedimentation (Supplementary Table S1). The settlement of colloids occurs at the micromodel bottom when the flow ceases before beginning two-phase flow. Conversely, the absence of energy minima at lower ionic strength and higher pH (for systems PS1 and PS3, Fig. 2a, and e) prevent the attachment of settled colloids in the porous media (due to RI). Consequently, those colloids remain suspended in bulk water and transported along with the moving fluid. However, as reported in previous studies, the charge variability or nanoscale surface roughness of the micromodel resulted in attachment of very few colloids even under repulsive conditions [39–42].

Therefore, understanding the favorability of colloid interaction with the SWI helps in predicting the dependence of colloid retention in porous media on solution chemistry. Visual findings from this study suggest that the interaction can be favorable between like-charged surfaces when the surface charge of the colloid is close to zero. On the other hand, unfavorable behavior of the colloids (i.e., similar to the hydrophobic colloids in this study) helps to modify the filtration efficiency by changing the solution chemistry accordingly. Moreover, it should be mentioned that the coupled impact of solution ionic strength and pH must be considered to enhance the removal of colloids from the pore scale for better performance of filters.

### 3.2. Colloid mobilization and retention in two-phase flow

Upon completion of single-phase experiments where saturation conditions were reached, drainage experiments were conducted by injecting $CO_2$ at a constant rate of 10 μL/min. Relative low initial colloid concentration (1.23%–4.41%, Table 1) and high porosity of the micromodel resulted in negligible changes in the $CO_2$ displacement patterns and residual water saturation in the micromodel. Therefore, residual water saturations determined from pore-scale images at REA were 54.8% (±4.6) in all experiments. Table 1 shows masses of colloids retained at residual water conditions as obtained from the images of REAs (Supplementary Fig. S1). Fig. 3 shows pore-scale images of size, 2.0 mm × 1.5 mm (i.e., 2127 × 1595 pixels) after drainage at different experimental conditions in this study. As observed from pore-scale images, deposited colloids in the micromodels at the start of drainage experiments were mobilized by the moving GWIs during two-phase flow. The mobilized colloids were attached to GWI and are either transported along with moving GWI or retained on stationary GWI in the pore space. A small amount of colloids was observed in the gas-phase, which are retained in thin films (Fig. 3b). Although colloids were not detached from GWI, their free movement along GWI resulted in retention on other retention sites, including Gas-Water–Solid Interface (GWSI) and thin water films. The random movement of colloids on GWI occurs due to Brownian motion or hydrodynamic forces, as reported in previous studies [3,47,48].

Table 1 gives ratios of the retained mass to the initial mass of colloids after drainage. This ratio (as percentages) ranged from 5.9% to 62.6% for hydrophobic colloids, whereas it ranged from 47.8% to 90% for hydrophilic colloids. Findings indicate that a substantial mass of hydrophobic colloids was detached and removed from the porous media compared to hydrophilic colloids during drainage. Similarly, the greater percentage of retention for both the colloids (62.6% for hydrophobic and 90% for hydrophilic) were found for the case of high ionic strength and low pH (PS4 and CMPS4, 100 mM and pH of 4). As can be seen from the data in Table 1, there is a clear trend of increasing colloid retention as ionic strength increased or as pH decreased upon the invasion of the GWI.

Table 1 shows the percentages of colloids remained on GWI in the pore space. This was approximately 20–30% higher for hydrophobic colloids compared to hydrophilic colloids. Moreover, for the case of high ionic strength and low pH, colloid mass retained on GWI was comparatively lesser than other cases (for PS4 61.4% and CMPS4 53.2%). The strong colloid-SWI interaction for hydrophilic colloids and colloids with greater ionic strength and smaller pH can explain their reduced retention on GWI. The higher affinity of colloids to SWI was reported in the previous literature due to the ionic strength and pH effect [2,6].

#### 3.2.1. Colloid-GWI interaction

Colloid retention on GWI was observed in all the experimental conditions irrespective of the type of colloids and solution chemistry, as shown in Fig. 3. Colloid retention occurs on GWI due to two types of interactions, namely hydrophobic interaction, HI, and capillary retention, CR.

HI is a retention mechanism where mobile colloids in the pore-space are retained on stationary GWIs. Whereas CR is another retention mechanism, where colloids deposited on SWI are mobilized due to GWIs movements. HI was observed for hydrophobic colloids only at low ionic strength and high pH conditions (Fig. 3a, and e). In contrast, CR was the dominant mechanism for colloid attachment on GWI and was observed in all experimental conditions, including those cases where HI was found (Table 2 and Fig. 3).

Relatively less retention was observed by HI as the mobile colloids transported through the connected flow path, and only a few colloids trapped in immobile water zones were available to interact with GWI, as observed from Fig. 3a, and e. As can be seen in Supplementary Movie 1 (Supporting materials), hydrodynamic forces in the stagnant water zones attract the colloids near to GWI, where colloids move along the GW interface. During the colloid movement near to GWI, the attachment to the GWI occurs when the contact time is greater than the time required for developing HI [43–45]. The reversal of the flow field (through the water film) near the solid surface distracts the moving colloids near GWI and prevents further interaction (Supplementary Movie 1-Supporting Material).

On the other hand, colloids retained on SWI at the start of the drainage experiments were detached by the moving GWI during drainage, as observed in Supplementary Movie 2 (Supporting Materials). When the moving GWI encounters deposited colloids, the interface deforms to form a three-phase contact line (Fig. 4). Considering the force balance (Fig. 4a), the vertical component of the capillary force exerted on the colloid lifted the colloids from SWI as it dominates over the adhesion force resulting in CR on GWI. CR was the primary retention mechanism on GWIs observed in this study irrespective of the type of colloid or solution chemistry. The CR of colloids can be utilized as an efficient mechanism for filter bed cleaning where the colloids retained on the collector surfaces mobilized and removed from the porous media by the passage of GWI.

#### 3.2.2. Colloid-GWSI interaction and thin film attachment

Fig. 5 shows pore-scale images of colloid retention on GWSI and thin films after drainage. GWSI and thin films around the solid surfaces (formed due to pore geometry, Fig. 4e) were visualized in these

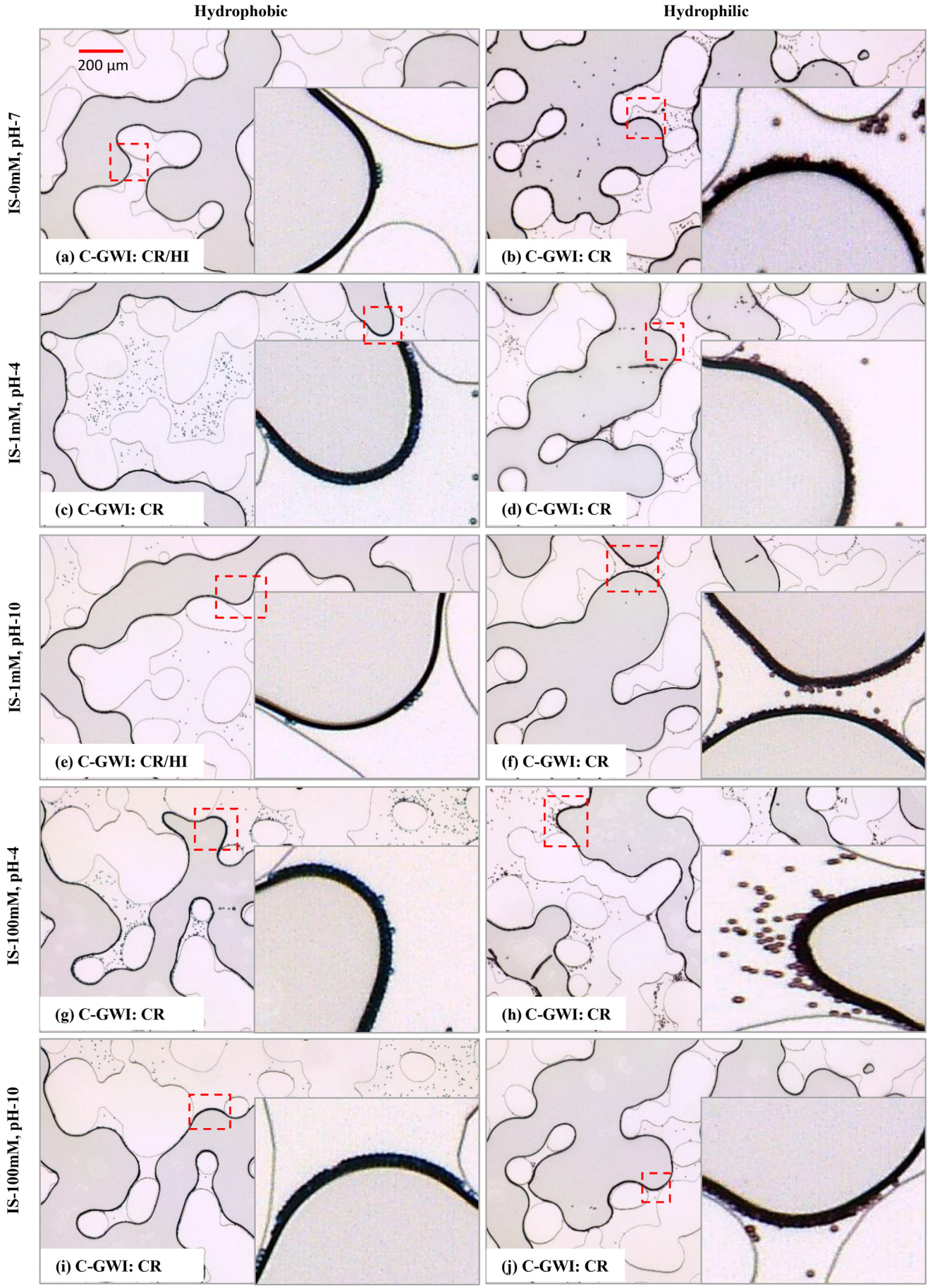


**Fig. 3.** Colloid interactions in Two-Phase flow at different experimental conditions; colloids interacting with GWI. CR: Capillary Retention, HI: Hydrophobic Interaction.

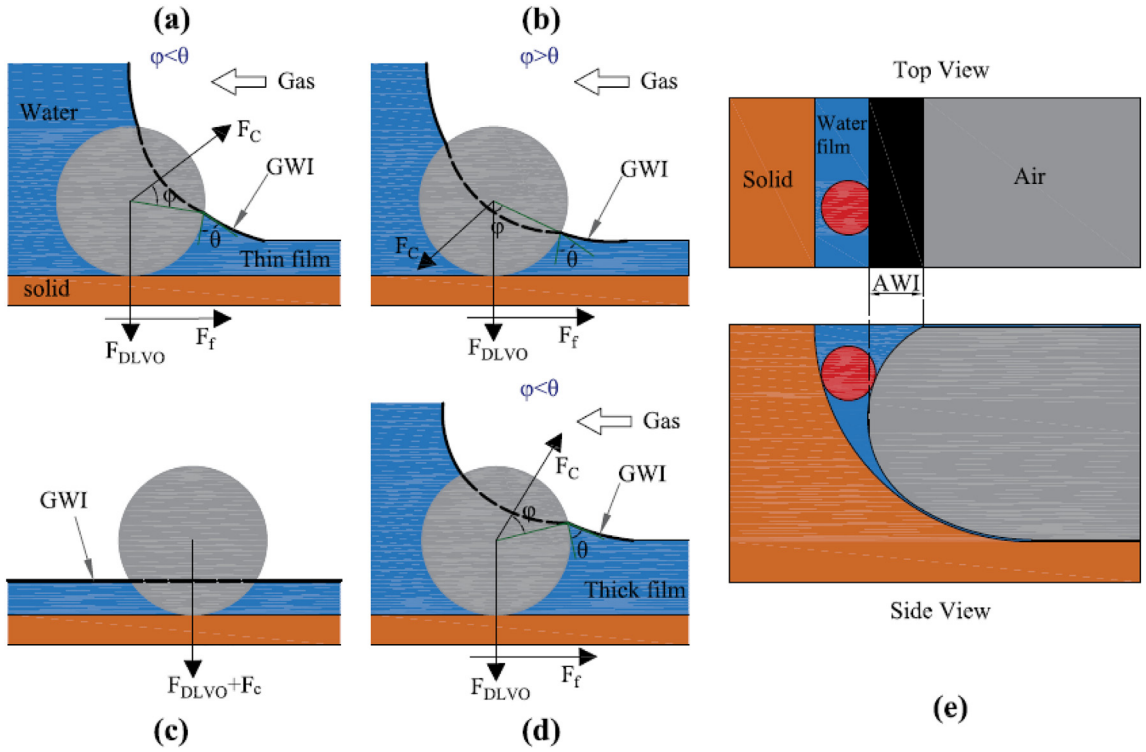


**Fig. 4.** Colloids interacting with drainage front. Capillary forces and DLVO forces are considered. Interface position on colloid (a) for GWI interaction; (b) for GWSI capillary retention; (c) thin-film attachment; (d) for GWSI straining; (e) thick water film formed around the solid surface due to the channel shape. φ is the angle determining the interface position on the colloid surface, and θ is the colloid contact angle.

experiments (Fig. 5). Two distinct types of colloid retention mechanisms were observed on GWSI in this study, namely straining, S, around the solid surfaces and capillary retention, CR, on GWSI, and thin films at the top and bottom of the micromodel. Straining was observed in all experimental conditions conducted in this study, whereas CR was observed for hydrophilic colloids and hydrophobic colloids only at higher ionic strength conditions (Fig. 5).

As can be seen in Supplementary Movie 2 (Supporting Material), colloids that are freely moving on GWI get trapped and immobilized near the solid phase. This observation was consistent with previous studies that reported the film thickness impacted the hydrodynamic drag near the solid boundary; colloids were trapped on thin films around the solid phase when the film thickness became less than the colloid diameter [46–48]. As measured from the captured images, film thickness approximately equals the colloid diameter (i.e., 5 μm). In such a case, colloids were trapped by a straining mechanism on the GWSI. Further invasion of GWI in the pore space led to straining on water films around the solid phase (e.g., Fig. 5a, c, and e). Straining of colloids on GWSI and water films were observed for all the experimental conditions in this study due to the rearrangement or alignment of colloids retained on GWI towards the solid surfaces. However, CR was feasible only when DLVO and capillary forces are strong enough to pin the colloids on SWI at GWSI. Therefore, all hydrophilic colloids and hydrophobic colloids only at higher ionic strength were experienced CR at GWSI and thin films near the top and bottom of the micromodel. On the other hand, hydrophobic colloids at low ionic strength experienced retention on GWSI and thin films by straining only, as shown in Fig. 5a, c, and e.

Unlike DLVO forces, capillary forces are independent of electrostatic characteristics and are affected by the colloid size, contact angle, and surface tension between two fluids. As can be seen in Fig. 5 and Table 2, higher CR was observed for hydrophilic colloids due to its greater capillary potential due to the impact of contact angle. As illustrated in Fig. 4b, the capillary force on a colloid at GWSI and the DLVO forces results in colloid pinning on GWSI. The frictional force on solid surface opposes the horizontal component of the capillary force, which tends to release the colloid back into bulk solution and thereby retain the colloid on GWSI. A solid-water contact angle greater than $45^0$ was not expected to retain the colloid on GWSI [49,50]. Nevertheless, pore-scale visualization revealed the pinning of GWI on SWI by the colloids, as seen in Fig. 5b, d, f, g, h, j, and i. This observation confirms the GWSI attachment in this study, where the average contact angle of the micromodel was 20°. However, for hydrophobic colloids at lower ionic strength, smaller or absence of adhesive forces (i.e., $\phi_{min1}$, Supplementary Table S1) with SWI prevents capillary pinning on GWSI or thin films. Therefore, the removal of colloids from the pore space of the porous media by the passage of GWI is an efficient mechanism for hydrophobic colloids at low ionic strength conditions.

Film thickness influences colloid interaction at GWSI and thin films as shown in Fig. 4b and d. Capillary pinning forces alter the interaction mechanisms from Straining to CR. Therefore, CR was not observed near the thick films formed around solid surfaces due to the micromodel channel shape (Fig. 5a, c, and e). As water film thickness was very small (less than 500 nm) at the top or bottom of the micromodel, CR was observed mostly between GWI and the top or bottom boundaries of the micromodel.

The possible conditions to occur thin-film CR were identified in this study based on the pore-scale observations. They are; (1) presence of excess colloids on GWI, (2) rapid invasion of the interface in the pore space, and (3) coalescence of two GWIs containing colloids. The excess colloids on GWI rearrange to GWSI under conditions (2) and (3) leaving them on thin films while the receding interface changes its position on the colloid, as shown in Fig. 4c. Consequently, capillary forces act together with adhesion forces to retain colloids in thin water films. Horizontal forces acting on the colloid at thin films were balanced in all directions and were permanently attached as long as the film exists. Therefore, the greater concentration of colloids in the porous media can cause thin-film CR and limit the removal or mobilization from

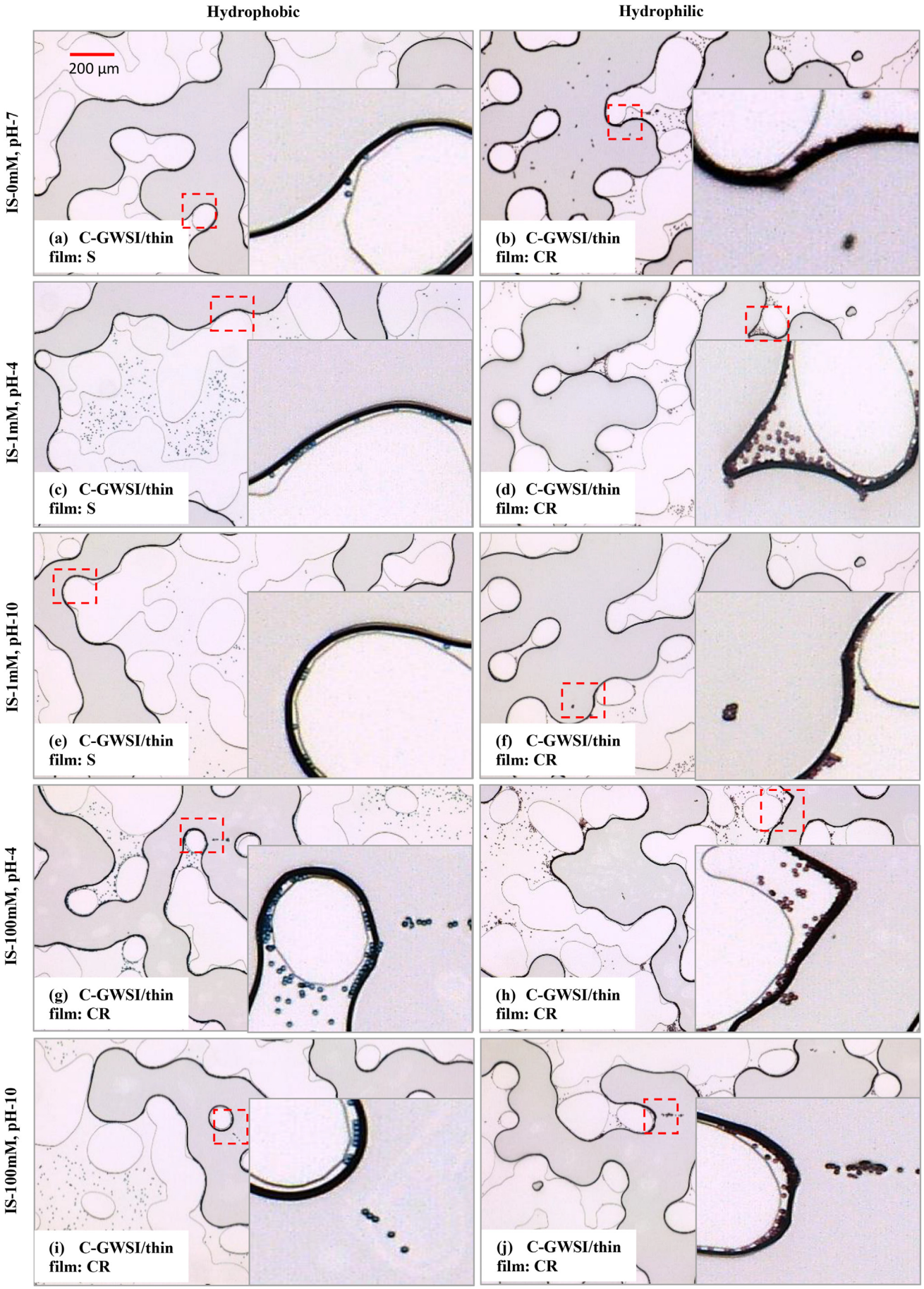


**Fig. 5.** Colloid interactions in Two-Phase flow at different experimental conditions; colloids interacting with GWSI/thin films. CR: Capillary Retention, S: Straining only.

porous media. To the best of our knowledge, this study is the first that explains possible conditions for thin-film attachment.

CR mechanism was more significant for hydrophilic colloids compared to hydrophobic colloids. This observation can be attributed to two possible factors: (1) a high capillary potential of hydrophilic colloids due to smaller contact angle along with strong adhesive forces on SWI, and (2) increased availability of colloids on GWI, which leads to film straining during GWI invasion of the pore space. Consequently, mobilization of the deposited colloids using GWI can be used effectively for hydrophobic colloids compared to hydrophilic colloids. Moreover, decreasing the ionic strength or increasing the pH of the solution before the GWI passage enhances the removal of colloids from porous media.

The behavior of colloids in single and two-phase flow systems was investigated in this study at different solid and fluid interfaces. However, there was no clear trend of changes in fluid displacement patterns and final $CO_2$ saturation for hydrophilic and hydrophobic colloids with the variation in solution chemistry. This is mainly due to the limited pore clogging that took place in the pore scape. Therefore, no significant changes were observed in the pore geometry due to the presence of colloids in the micromodel to influence the fluid displacement pattern and residual saturation. Limited pore clogging was attributed to the following reasons: (1) low colloid concentration used in this study due to experimental limitations (i.e., to avoid micromodel inlet clogging at high colloid concentration); (2) large porosity of the micromodel (i.e., 58%); and (3) small colloid size (i.e., 5 μm, which was smaller than the smaller pore throat size of the porous media, i.e., 20 μm).

## 4. Conclusions

In this study, pore-scale experiments were conducted to investigate the coupled effects of ionic strength and pH of the solution, and colloid hydrophobicity on colloid retention and mobilization mechanisms in porous media. Microfluidic systems were used to conduct single and two-phase flow experiments at different conditions. Main findings of this study are:

1. In single-phase flow conditions, significant retention of colloids was observed for hydrophilic colloids due to long-range interaction of colloids with solid-water-interfaces and long-range/short-range interactions with other colloids. However, repulsive interactions were dominant for hydrophobic colloids, which impede their filtration in porous media.
2. For hydrophobic colloids, changes in solution chemistry (i.e., an increase in ionic strength or decrease in pH) significantly increased colloid interactions with other colloids or solid-water-interface. At these conditions (i.e., high ionic strength or low pH), it was observed that short-range interactions and long-range interactions were the dominant retention mechanisms. However, the impact of solution chemistry was insignificant for hydrophilic colloids.
3. In two-phase flow conditions, colloids that were deposited on solid-water interfaces were mobilized by the moving gas-water interface and then were attached to the gas-water interfaces due to capillary retention. This mobilization can be effectively utilized to clean filter beds where the deposited colloids can be removed from the porous media.
4. In two-phase flow conditions, hydrophobic colloids mobilize easily by the gas-water interface and can be effectively removed from the porous media. On the other hand, colloids on gas-water interface redeposit on the gas-water-solid interface or thin water films for hydrophilic colloids due to their greater capillary potential.
5. As the ionic strength increases or the pH of the solution decreases, colloid interaction with solid-water interface strengthen, which in turn reduces colloid mobilization by gas-water interfaces for hydrophobic and hydrophilic colloids.
6. Findings indicate that the coupled effects of solution chemistry and colloid hydrophobicity must be investigated to better understand colloid retention mechanisms.

Therefore, greater filtration efficiency can be achieved with the hydrophilic colloids compared to the hydrophobic colloids for which the efficiency can be improved by changing the solution chemistry. Moreover, the removal of colloids deposited on the filter bed can be achieved by the passage of GWI. The removal efficiency was observed to be more for hydrophobic colloids compared to hydrophilic colloids for which the efficiency can be improved by lowering the ionic strength or increasing the pH. Hence understanding the interaction mechanisms helps to design efficient filters and suggest techniques for efficient cleaning practices.

## Declaration of Competing Interest

The authors declare that they have no known competing financial interests or personal relationships that could have appeared to influence the work reported in this paper.

## Acknowledgment

Open Access funding provided by the Qatar National Library. This publication was made possible by partial funding from NPRP grant #NPRP8-594-2-244 from the Qatar National Research Fund (a member of Qatar Foundation). Any opinions, findings, and conclusions or recommendations expressed in this material are those of the authors and do not necessarily reflect the view of funding agencies. Safna Nishad was funded by the Graduate Assistantship program at Qatar University. The authors would like to thank the Center for Advanced Materials (CAM) at Qatar University for help in Zeta Potential Analysis.

## Appendix A. Supplementary data

Supplementary data to this article can be found online at https://doi.org/10.1016/j.powtec.2020.08.086.

## References

[1] T. Waller, I.M. Marcus, S.L. Walker, Influence of septic system wastewater treatment on titanium dioxide nanoparticle subsurface transport mechanisms, Anal. Bioanal. Chem. 410 (2018) 6125–6132.
[2] R.H. Morin, D.R. LeBlanc, B.M. Troutman, The influence of topology on hydraulic conductivity in a sand-and-gravel aquifer, Groundwater. 48 (2010) 181–190.
[3] V.I. Syngouna, C.V. Chrysikopoulos, Experimental investigation of virus and clay particles cotransport in partially saturated columns packed with glass beads, J. Colloid Interface Sci. 440 (2015) 140–150.
[4] K.R. Bradbury, M.A. Borchardt, M. Gotkowitz, S.K. Spencer, J. Zhu, R.J. Hunt, Source and transport of human enteric viruses in deep municipal water supply wells, Environ. Sci. Technol. 47 (2013) 4096–4103.
[5] Z. Mesticou, M. Kacem, P. Dubujet, Influence of ionic strength and flow rate on silt particle deposition and release in saturated porous medium: experiment and modeling, Transp. Porous Media 103 (2014) 1–24.
[6] Q. Zhang, S.M. Hassanizadeh, B. Liu, J.F. Schijven, N.K. Karadimitriou, Effect of hydrophobicity on colloid transport during two-phase flow in a micromodel, Water Resour. Res. 50 (2014) 7677–7691.
[7] H.-J. Kim, T. Phenrat, R.D. Tilton, G.V. Lowry, Effect of kaolinite, silica fines and pH on transport of polymer-modified zero valent iron nano-particles in heterogeneous porous media, J. Colloid Interface Sci. 370 (2012) 1–10, https://doi.org/10.1016/j.jcis.2011.12.059.
[8] P.N. Mitropoulou, V.I. Syngouna, C.V. Chrysikopoulos, Transport of colloids in unsaturated packed columns: role of ionic strength and sand grain size, Chem. Eng. J. 232 (2013) 237–248, https://doi.org/10.1016/j.cej.2013.07.093.
[9] S. Aramrak, M. Flury, J.B. Harsh, Detachment of deposited colloids by advancing and receding air–water interfaces, Langmuir. 27 (2011) 9985–9993.
[10] S. Aramrak, M. Flury, J.B. Harsh, R.L. Zollars, Colloid mobilization and transport during capillary fringe fluctuations, Environ. Sci. Technol. 48 (2014) 7272–7279.
[11] V. Lazouskaya, L.-P. Wang, D. Or, G. Wang, J.L. Caplan, Y. Jin, Colloid mobilization by fluid displacement fronts in channels, J. Colloid Interface Sci. 406 (2013) 44–50.
[12] P. Sharma, M. Flury, J. Zhou, Detachment of colloids from a solid surface by a moving air-water interface, J. Colloid Interface Sci. 326 (2008) 143–150, https://doi.org/10.1016/j.jcis.2008.07.030.
[13] V. Lazouskaya, L.-P. Wang, H. Gao, X. Shi, K. Czymmek, Y. Jin, Pore-scale investigation of colloid retention and mobilization in the presence of a moving air–water interface, Vadose Zo. J. 10 (2011) 1250–1260.
[14] Q. Zhang, A. Raoof, S.M. Hassanizadeh, Pore-scale study of flow rate on colloid attachment and remobilization in a saturated micromodel, J. Environ. Qual. 44 (2015) 1376–1383.

[15] Q. Zhang, S.M. Hassanizadeh, The role of interfacial tension in colloid retention and remobilization during two-phase flow in a polydimethylsiloxane micro-model, Chem. Eng. Sci. 168 (2017) 437–443.
[16] Y. Guo, J. Huang, F. Xiao, X. Yin, J. Chun, W. Um, Bead-Based Microfluidic Sediment Analogues: Fabrication and Colloid Transport, 2016https://doi.org/10.1021/acs.langmuir.6b02184.
[17] G.C. Agbangla, É. Climent, P. Bacchin, Experimental investigation of pore clogging by microparticles: evidence for a critical flux density of particle yielding arches and deposits, Sep. Purif. Technol. 101 (2012) 42–48.
[18] J. Jung, S. Cao, R. Al-Raoush, K. Alshibli, Fines migration and clogging behavior in methane hydratebearing sediments, Qatar Found. Annu. Res. Conf. Proc. 2018 (2018), EEPD710. https://doi.org/10.5339/qfarc.2018.EEPD710.
[19] J. Jung, S.C. Cao, Y.-H. Shin, R.I. Al-Raoush, K. Alshibli, J.-W. Choi, A microfluidic pore model to study the migration of fine particles in single-phase and multi-phase flows in porous media, Microsyst. Technol. (2017) https://doi.org/10.1007/s00542-017-3462-1.
[20] M. Auset, A.A. Keller, Pore-scale visualization of colloid straining and filtration in saturated porous media using micromodels, 42 (2006) 1–9, https://doi.org/10.1029/2005WR004639.
[21] E. Dressaire, A. Sauret, Clogging of microfluidic systems, Soft Matter 13 (2017) 37–48.
[22] V. Lazouskaya, Y. Jin, Colloid retention at air–water interface in a capillary channel, Colloids Surf. A Physicochem. Eng. Asp. 325 (2008) 141–151, https://doi.org/10.1016/j.colsurfa.2008.04.053.
[23] V. Lazouskaya, Y. Jin, D. Or, Interfacial interactions and colloid retention under steady flows in a capillary channel, J. Colloid Interface Sci. 303 (2006) 171–184, https://doi.org/10.1016/j.jcis.2006.07.071.
[24] Q. Zhang, S.M. Hassanizadeh, N.K. Karadimitriou, A. Raoof, B. Liu, P.J. Kleingeld, A. Imhof, Retention and remobilization of colloids during steady-state and transient two-phase flow, Water Resour. Res. 49 (2013) 8005–8016.
[25] W. Song, A.R. Kovscek, Functionalization of micromodels with kaolinite for investigation of low salinity oil-recovery processes, Lab Chip 15 (2015) 3314–3325, https://doi.org/10.1039/C5LC00544B.
[26] W. Song, A.R. Kovscek, Direct visualization of pore-scale fines migration and formation damage during low-salinity waterflooding, J. Nat. Gas Sci. Eng. 34 (2016) 1276–1283, https://doi.org/10.1016/j.jngse.2016.07.055.
[27] W. Wang, S. Chang, A. Gizzatov, Toward reservoir-on-a-chip: fabricating reservoir micromodels by in situ growing calcium carbonate nanocrystals in microfluidic channels, ACS Appl. Mater. Interfaces 9 (2017) 29380–29386.
[28] Y.A. Alzahid, P. Mostaghimi, A. Gerami, A. Singh, K. Privat, T. Amirian, R.T. Armstrong, Functionalisation of polydimethylsiloxane (PDMS)-microfluidic devices coated with rock minerals, Sci. Rep. 8 (2018) 15518.
[29] T. Amirian, M. Haghighi, P. Mostaghimi, Pore scale visualization of low salinity water flooding as an enhanced oil recovery method, Energy Fuel 31 (2017) 13133–13143.
[30] S.C. Cao, S. Dai, J. Jung, Supercritical $CO_2$ and brine displacement in geological carbon sequestration: micromodel and pore network simulation studies, Int. J. Greenh. Gas Control. 44 (2016) 104–114, https://doi.org/10.1016/j.ijggc.2015.11.026.
[31] M. Kim, A. Abedini, P. Lele, A. Guerrero, D. Sinton, Microfluidic pore-scale comparison of alcohol-and alkaline-based SAGD processes, J. Pet. Sci. Eng. 154 (2017) 139–149.
[32] Y.A. Alzahid, P. Mostaghimi, S.D.C. Walsh, R.T. Armstrong, Flow regimes during surfactant flooding: the influence of phase behaviour, Fuel. 236 (2019) 851–860.
[33] J.T. Crist, Y. Zevi, J.F. McCarthy, J.A. Throop, T.S. Steenhuis, Transport and retention mechanisms of colloids in partially saturated porous media, Vadose Zo. J. 4 (2005) 184–195.
[34] E. Joseph, G. Singhvi, Multifunctional nanocrystals for cancer therapy: a potential nanocarrier, Nanomaterials for Drug Delivery and Therapy, Elsevier 2019, pp. 91–116.
[35] A. Kumar, C.K. Dixit, Methods for characterization of nanoparticles, Advances in Nanomedicine for the Delivery of Therapeutic Nucleic Acids, Elsevier 2017, pp. 43–58.
[36] S. Torkzaban, S.A. Bradford, J.L. Vanderzalm, B.M. Patterson, B. Harris, H. Prommer, Colloid release and clogging in porous media: effects of solution ionic strength and flow velocity, J. Contam. Hydrol. 181 (2015) 161–171.
[37] S. Torkzaban, H.N. Kim, J. Simunek, S.A. Bradford, Hysteresis of colloid retention and release in saturated porous media during transients in solution chemistry, Environ. Sci. Technol. 44 (2010) 1662–1669.
[38] J.J. Lenhart, J.E. Saiers, Colloid mobilization in water-saturated porous media under transient chemical conditions, Environ. Sci. Technol. 37 (2003) 2780–2787.
[39] C. Jin, T. Glawdel, C.L. Ren, M.B. Emelko, Non-linear, non-monotonic effect of nanoscale roughness on particle deposition in absence of an energy barrier: experiments and modeling, Sci. Rep. 5 (2015) 17747.
[40] P. Zhang, B. Bai, S. Jiang, P. Wang, H. Li, Transport and deposition of suspended particles in saturated porous media: effect of hydrodynamic forces and pore structure, Water Sci. Technol. Water Supply 16 (2016) 951–960.
[41] W.P. Johnson, X. Li, G. Yal, Colloid retention in porous media: mechanistic confirmation of wedging and retention in zones of flow stagnation, Environ. Sci. Technol. 41 (2007) 1279–1287.
[42] W.P. Johnson, M. Hilpert, Upscaling colloid transport and retention under unfavorable conditions: linking mass transfer to pore and grain topology, Water Resour. Res. 49 (2013) 5328–5341.
[43] B. Albijanic, O. Ozdemir, A.V. Nguyen, D. Bradshaw, A review of induction and attachment times of wetting thin films between air bubbles and particles and its relevance in the separation of particles by flotation, Adv. Colloid Interf. Sci. 159 (2010) 1–21.
[44] P. Knüpfer, J. Fritzsche, T. Leistner, M. Rudolph, U.A. Peuker, Investigating the removal of particles from the air/water-interface–Modelling detachment forces using an energetic approach, Colloids Surf. A Physicochem. Eng. Asp. 513 (2017) 215–222.
[45] N. Ishida, Direct measurement of hydrophobic particle–bubble interactions in aqueous solutions by atomic force microscopy: effect of particle hydrophobicity, Colloids Surf. A Physicochem. Eng. Asp. 300 (2007) 293–299.
[46] D.F. Williams, J.C. Berg, The aggregation of colloidal particles at the air—water interface, J. Colloid Interface Sci. 152 (1992) 218–229.
[47] D. Ershov, J. Sprakel, J. Appel, M.A.C. Stuart, J. van der Gucht, Capillarity-induced ordering of spherical colloids on an interface with anisotropic curvature, Proc. Natl. Acad. Sci. 110 (2013) 9220–9224.
[48] S. Das, J. Koplik, R. Farinato, D.R. Nagaraj, C. Maldarelli, P. Somasundaran, The translational and rotational dynamics of a colloid moving along the air-liquid interface of a thin film, Sci. Rep. 8 (2018) 8910.
[49] Y. Zevi, A. Dathe, B. Gao, W. Zhang, B.K. Richards, T.S. Steenhuis, Transport and retention of colloidal particles in partially saturated porous media: effect of ionic strength, Water Resour. Res. 45 (2009).
[50] B. Gao, T.S. Steenhuis, Y. Zevi, V.L. Morales, J.L. Nieber, B.K. Richards, J.F. McCarthy, J. Parlange, Capillary retention of colloids in unsaturated porous media, Water Resour. Res. 44 (2008).